Numerical Computation on Recirculation Flow Structures in Co-Axial Confined Laminar Jets

P. L. WOODFIELD, K. NAKABE and K. SUZUKI,
Heat Transfer Laboratory, Department of Mechanical Engineering, Kyoto University,
Kyoto 606-8501, Japan
E-mail: pwoodf@ip.media.kyoto-u.ac.jp

'Craya-Curtet' number (*Ct*) has been described as one of the most suitable universal similarity parameters for co-axial confined jets. This work shows that the formation of the recirculation zone is greatly influenced by Reynolds number, and not by Ct alone under laminar flow conditions. If the length scale of the thermo-fluid machinery is decreased, for example, in micro jet flame combustors, the corresponding Reynolds number, Re, becomes smaller. In the case of Re > 50, the length of the recirculation zone is found proportional to Re number for a fixed value of Ct. In the limit of very small Re number, the recirculation zone disappears, unlike turbulent flow cases.

1. Introduction

Fundamental investigation into confined jet interactions at low Reynolds number has particular value for the development of micro-jet pumps and micro combustors. The co-axial confined jet, which is perhaps one of the simplest possible configurations, was selected for this study.

Figure 1 gives a schematic illustration for the computational domain. Under certain conditions where the momentum of the primary (center) jet is sufficiently in excess of the momentum of the secondary (annular) jet, an axisymmetric recirculation zone appears on the wall of the tube as shown in the figure.

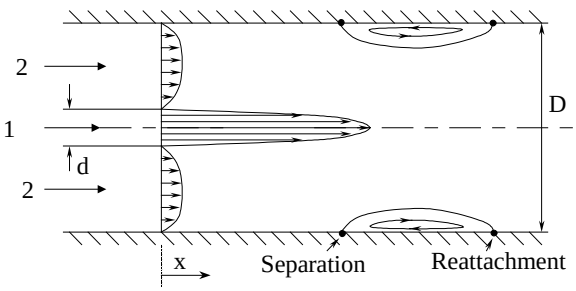

Fig. 1 Co-axial confined jet configuration (1: Primary jet; 2: Secondary jet. Inlet velocity profiles are the fully developed laminar profiles for circular and annular tubes).

For the present work, Reynolds number is based on the mean velocity, *U*, averaged over the entire tube cross-section and on the diameter of the tube, *D*.

2. Mathematical Model

In order to consider the simplest case, the flow is taken to be steady and laminar. All fluid properties are assumed constant. Governing equations for axial and radial momentum are solved together with the continuity equation.

Equations 1 and 2 give the Navier-Stokes equations for conservation of momentum.

$$\rho u\frac{\partial u}{\partial x}+\rho v\frac{\partial u}{\partial r}=\mu\frac{\partial^2 u}{\partial x^2}+\frac{\mu}{r}\frac{\partial}{\partial r}\left(r\frac{\partial u}{\partial r}\right)-\frac{\partial p}{\partial x} \quad \ldots(1)$$

$$\rho u\frac{\partial v}{\partial x}+\rho v\frac{\partial v}{\partial r}=\mu\frac{\partial^2 v}{\partial x^2}+\mu\frac{\partial}{\partial r}\left(\frac{1}{r}\frac{\partial rv}{\partial r}\right)-\frac{\partial p}{\partial r} \quad \ldots(2)$$

Equation 3 gives the constant property continuity equation in cylindrical coordinates.

$$\frac{\partial u}{\partial x}+\frac{1}{r}\frac{\partial}{\partial r}(rv)=0 \quad \ldots(3)$$

3. Boundary Conditions

The inlet velocity profiles are for fully developed tube flow (primary stream) and fully developed annular flow (secondary stream) as shown in Fig. 1. The radial velocity component is zero over the entire inlet cross-section (i.e. at x = 0). The computational domain extends to 33 tube diameters downstream of the inlet, and a zero normal gradient boundary condition is assumed at the exit.

4. Numerical Technique

For the solution of Eqs. (1) to (3), the method of finite volumes is used in conjunction with Patankar's SIMPLE technique[1]. For the discretization of the convection and diffusion terms, a first-order hybrid differencing scheme is employed[1]. Code validation was performed by comparison with fully developed pipe flow data and experimental velocity distributions for the confined laminar jet by Shavit and Lavan[2].

A computational grid of 200 by 54 cells ($x\times r$) is used to discretize the domain, the grid spacing being progressively finer closer to the inlet. For the very low Reynolds number calculations (Re<10), the length of the computational domain is reduced whilst maintaining the same number of grid points to preserve the fine resolution.

5. Effect of Craya-Curtet Number

The Craya-Curtet number is a well-known similarity parameter for

the co-axial confined turbulent jet. In the present work the effect of this parameter upon the confined laminar jet is examined. The definition of *Ct* used[3], is given in Eqs. (4) to (6).

$$C_t = \frac{U_o}{\sqrt{U_d^2 - 0.5U_o^2}} \qquad \ldots(4)$$

$$U_d^2 = \frac{1}{A_o}\int_{A_o}(u^2 - 0.5U_f^2)dA \qquad \ldots(5)$$

$$U_o = \frac{1}{A_o}\int_{A_o} u dA \qquad \ldots(6)$$

For the turbulent case, U_f is defined as the inlet velocity at the constant velocity part of the co-current stream. Here it is taken to be the mean velocity of the co-current stream as given in Eq. (7). To maintain consistency with this assumption, when evaluating the integral in Eq. (5), it is also assumed that the velocity profile is flat over the entire secondary stream at the entrance. For the present calculations, the effect of the secondary stream profile is found to be small giving some justification to this assumption.

In Eqs. (5) - (7), 'A_o' is the entire cross-sectional area of the tube and 'A_2' is the cross-sectional area of the secondary stream at the entrance (i.e. 'A_o' minus the primary jet cross-sectional area).

$$U_f = U_2 = \frac{1}{A_2}\int_{A_2} u dA \qquad \ldots(7)$$

Figure 2 shows the effect of Craya-Curtet number on the flow field for a Reynolds number of 50. For all three cases in Fig. 2, the mass flow rates of the two streams are kept constant, the ratio of the primary flow to the secondary flow (m_1/m_2) being 0.32. The Craya-Curtet number is altered by adjusting the diameter of the primary jet. For a smaller diameter and the same flow rate, the momentum of the primary jet increases and hence *Ct* decreases.

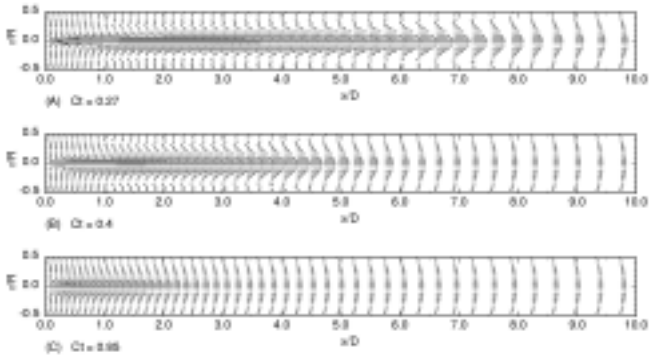

Fig. 2 Effect of *Ct* on flow field (Re = 50, m_1/m_2 = 0.32, Craya-Curtet number is altered by varying the nozzle diameter of the primary jet. (A) *d/D* = 0.074; (B) *d/D* = 0.111; (C) *d/D* = 0.222. Mass flow-rates of the two streams are the same for all three cases. Reynolds number is calculated on mean axial velocity and the diameter of the tube).

In Fig. 2 (A) and (B), a weak recirculation zone appears on the tube wall. In case (C) of Fig. 2 with *Ct* = 0.85, the recirculation does not appear. This is consistent with observations by Curtet and others of the turbulent case where for *Ct* less than about 0.75 recirculation occurs downstream of the inlet on the duct wall.[3,4] (It should be noted however, that the critical value of *Ct* for which the recirculation appears, reported in the literature, ranges from 0.75 to 0.976).[3]

Figure 3 shows the effect of the Craya-Curtet number on the friction coefficient at the wall. The three curves represent the three cases given in the previous figure (Fig. 2) for a Reynolds number of 50. 'C_f' is defined as given in Eq. (8).

$$C_f \equiv \frac{\tau}{\rho U^2/2} \qquad \ldots(8)$$

For fully developed flow, C_f takes on a value of 16/Re which agrees to within 0.05% of the calculated downstream values shown in Fig. 3.

At the mixing zone entrance (i.e. at x = 0), the wall friction coefficient increases slightly as the diameter of the primary jet is increased. This is because the secondary and primary mass flow rates are the same for the three cases, and hence the velocities in the secondary annular jet increase as the cross-sectional area is shrunken following the increase of the primary jet area.

The points where the curves intercept the *x*-axis correspond to the separation and reattachment points for the recirculation zone. Quite clearly in Fig. 3, the separation point moves only slightly upstream with a decrease in Craya-Curtet number from 0.4 to 0.27. The reattachment point, on the other hand, is affected drastically by *Ct* moving from about 4.5 tube diameters downstream of the entrance to about 8 tube diameters as *Ct* is varied from 0.4 to 0.27. This is quite different to the turbulent case where the reattachment point moves only slightly as *Ct* is decreased and the separation point moves remarkably upstream as *Ct* is decreased.

Also, all three curves in Fig. 3, display a minimum (or maximum negative) friction coefficient located at a point which moves downstream as *Ct* is decreased.

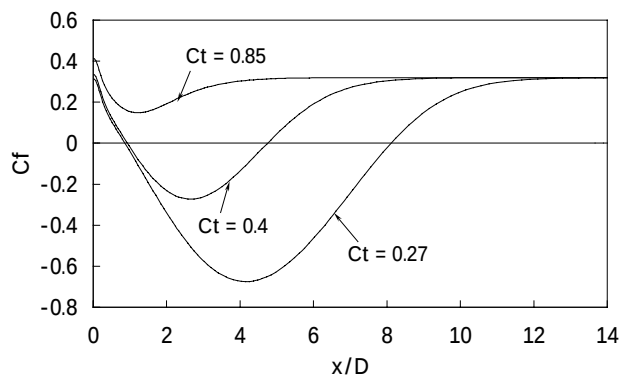

Fig. 3 Wall friction coefficient – Effect of *Ct* (Re = 50 and m_1/m_2 = 0.32).

6. Effect of Reynolds Number

For the case of the developing flow in a tube, the 'hydrodynamic entry length' extends approximately in proportion to Reynolds number. This proportionality breaks down if the flow becomes turbulent or under creeping flow conditions.[5] Also, for the case of

the sudden expansion duct, the reattachment point of the eddy forming in an axisymmetric backward facing step moves downstream in proportion to Reynolds number.[6] Macagno and Hung[6] found the distance to the reattachment point to be almost directly proportional to Reynolds number between 40 and 200 and curving upward slightly for Re < 40 in which Re is based on the diameter and mean velocity of the smaller duct).

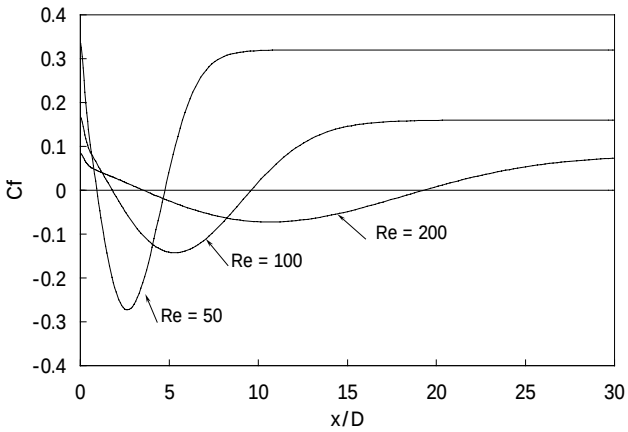

Fig. 4 Wall friction coefficient – Effect of Reynolds number (*Ct* = 0.4 and m_1/m_2 = 0.32).

The same kind of proportionality with respect to Reynolds number is observed here for the case of the axisymmetric confined laminar jet. Figure 4 shows the skin friction coefficient at the wall for the cases of Re = 50, 100 and 200 where the relative proportion of the primary and secondary fluid flow is kept constant. The ratio of *d/D* is also constant so that *Ct* is the same for all three cases.

Quite clearly in Fig. 4, for the range of Reynolds number investigated, the distances to both the separation and reattachment points increase in the downstream direction in a virtually linear proportion with Reynolds number. This point is further highlighted in Fig. 5. Here, the *x*-coordinates are divided by Reynolds number, and the skin friction coefficient is normalized with respect to the value for fully developed tube flow (16/Re). The three curves are remarkably similar with a slightly closer correlation for the cases of Re = 100 and 200.

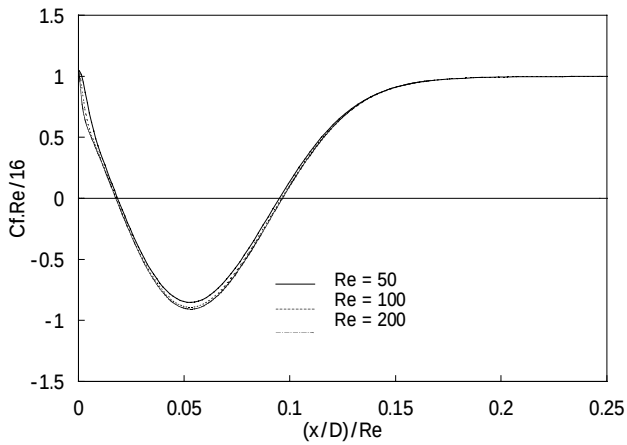

Fig. 5 Normalized skin friction coefficient – Relation to Reynolds number (*Ct* = 0.4 and m_1/m_2 = 0.32).

The close matching of the curves in Fig. 5 suggests a strong correlation between the velocity profiles at points located with the same value of *x/(D.Re)*. Figure 6 compares the dimensionless axial velocity distributions at various points for Re = 50 and 200, downstream in the axial direction having the same value for *x/(D.Re)*. In this figure, the solid lines are for a Reynolds number of 50 and the dashed lines are for a Reynolds number of 200. At almost all of the positions considered, the agreement between the two cases is so close that it is difficult to distinguish between the two lines. Even at the axial position '*C*', which is located approximately half way between the separation and reattachment points, the agreement for the reverse flow is also very close.

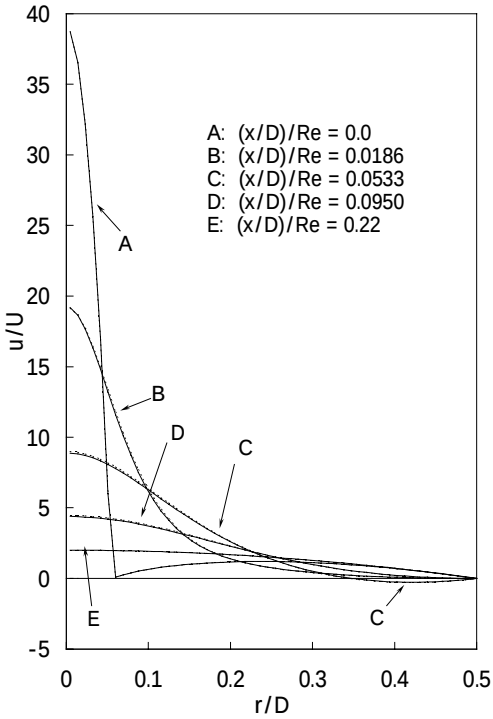

Fig. 6 Axial velocity distributions (*Ct* = 0.4, m_1/m_2 = 0.32, Re = 50 (solid lines) and Re = 200 (dashed lines)).

Having obtained such a close correlation for dimensionless axial velocities, *u/U*, with respect to the dimensionless coordinate, *x/(D.Re)*, mass conservation would suggest that there will be some similarity for the radial component of velocity for different Reynolds number and the same Craya-Curtet number. Figure 7 gives the dimensionless radial velocity *(v/U).Re* in terms of axial coordinate, *x/(D.Re)* for four different radial positions. Again there can be seen a clear correlation between the two Reynolds number cases except the largest differences in the near entrance region.

It is also apparent from Fig. 7 that the close matching of the radial velocity curves applies at different radial positions across the diameter of the tube. In Fig. 7, the position '*A*' (*r/D* = 0.042) is inside the primary jet (cf. *(d/2)/D* = 0.055) and hence the radial component is positive for all downstream values of *x*, tending to zero as *x* becomes large. The positions '*B*' and '*C*' begin outside the primary jet and hence the radial velocity takes on relatively large negative values just downstream of the entrance, increasing in closer proximity to the jet. A little further downstream, the jet width grows to coincide with the radial positions '*B*' and '*C*' and hence the velocities become positive. As the radial distance from the jet center is increased, the influence of the jet upon the radial velocity diminishes as shown by the line for position '*D*' in Fig. 7.

For all radial positions, the boundary condition at $x = 0$ is that $v = 0$. Because of the scaling and the large jump in radial velocity immediately downstream of the entrance this is a little difficult to decipher from Fig. 7. In fact, this sudden jump in the radial velocity profile calls into question the practical possibility of the zero radial velocity inlet boundary condition. The radial velocity distribution within the jets upstream of the entrance to the mixing region may in fact be influenced by the downstream conditions. Hence, as suggested by Shavit and Lavan[2], ideally the computational domain should be extended a little upstream of the jet nozzle exit.

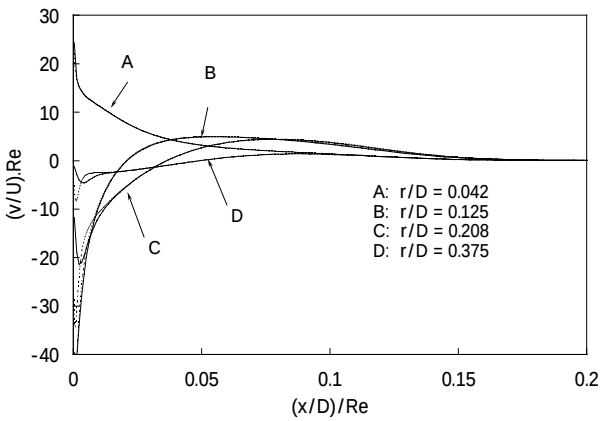

Fig. 7 Dimensionless radial velocity distributions (Ct = 0.4, m_1/m_2 = 0.32, Re = 50 (solid lines) and Re = 200 (dashed lines)).

7. Low Reynolds Number Limit

Figure 8 gives the normalized skin friction coefficient against the dimensionless axial distance, *x/(D.Re)*, for low Reynolds number (1 < Re < 200) and a fixed Craya-Curtet number (*Ct* = 0.4). As Reynolds number is reduced to below 30, the proportionality of the eddy size with respect to Reynolds number diminishes, although the remarkable similarity was shown in Fig. 5 for the cases, 50 < Re < 200. Between the cases of Re = 10 and 5, the recirculation zone vanishes altogether. If the flow rate is reduced even further to a Reynolds number of 2, the location of the minimum value for C_f moves downstream with respect to the dimensionless distance, *x/(D.Re)*.

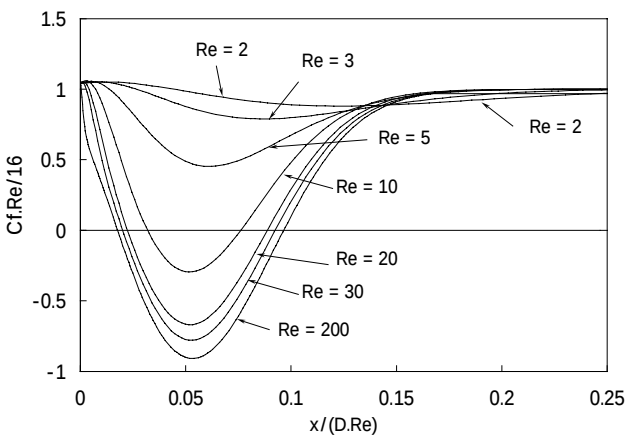

Fig. 8 Normalized skin friction coefficient – Effect of further reducing Reynolds number (*Ct* = 0.4 for all cases).

This result is consistent with the experimental findings of other researchers for the case of developing laminar flow in a tube where the proportional lengthening of the flow field with respect to Reynolds number diminishes as Reynolds number becomes very small[5]. Macagno and Hung[6] made the same observation results in the case of a sudden expansion duct.

It is interesting to note here, that for the case of Re < 10 in Fig. 8, the length of the recirculation zone is less than one tube diameter.

8. Discussion

The expansion of the flow field in approximate proportion to Reynolds number shown in Figs. 4 to 7 can be explained in part by non-dimensionalizing the constant property Navier-Stokes equations in terms of the following dimensionless parameters.

$$x^* = \frac{x}{D.\mathrm{Re}} \qquad r^* = \frac{r}{D} \qquad u^* = \frac{u}{U}$$
$$v^* = \frac{v}{U} \times \mathrm{Re} \qquad p^* = \frac{p}{\rho U^2} \qquad t^* = \frac{t.U}{D.\mathrm{Re}} \qquad \ldots(9)$$

In terms of these dimensionless groups, the boundary conditions for the three examples given in Figs. 4 to 7 are identical.

This particular scheme used here for non-dimensionalization is almost similar to the one proposed by Pai and Hsieh[7] (1972), which produces two-dimensional 'boundary layer' type equations (independent of Reynolds number) suitable for analysis of laminar jets with and without free stream. Moreover, Langhaar[8] (1942), for the analysis of developing flow in a tube, used *x/(a.Re)* for the dimensionless axial coordinate (where 'a' is the radius of the tube).

Using the above transformations the Navier-Stokes equations, Eq. (1) and (2) become as follows:

$$\frac{\partial u^*}{\partial t^*} + u^* \frac{\partial u^*}{\partial x^*} + v^* \frac{\partial u^*}{\partial r^*} = \frac{1}{\mathrm{Re}^2}\frac{\partial^2 u^*}{\partial x^{*2}} + \frac{1}{r^*}\frac{\partial}{\partial r^*}\left(r^* \frac{\partial u^*}{\partial r^*}\right) - \frac{\partial p^*}{\partial x^*} \qquad \ldots(10)$$

$$\frac{\partial v^*}{\partial t^*} + u^* \frac{\partial v^*}{\partial x^*} + v^* \frac{\partial v^*}{\partial r^*} = \frac{1}{\mathrm{Re}^2}\frac{\partial^2 v^*}{\partial x^{*2}} + \frac{\partial}{\partial r^*}\left(\frac{1}{r^*}\frac{\partial}{\partial r^*}(r^* v^*)\right) - \mathrm{Re}^2 \frac{\partial p^*}{\partial r^*} \qquad \ldots(11)$$

The time dependent terms are retained here to show that the analysis will be applied also to the unsteady case.

The continuity equation (Eq. (3)) transforms very simply into the following equation.

$$\frac{\partial u^*}{\partial x^*} + \frac{1}{r^*}\frac{\partial}{\partial r^*}\left(r^* v^*\right) = 0 \qquad \ldots(12)$$

In Eqs. (10) to (12), there are three terms which still contain Reynolds number:

$$\frac{1}{\mathrm{Re}^2}\frac{\partial^2 u^*}{\partial x^{*2}}, \quad \frac{1}{\mathrm{Re}^2}\frac{\partial^2 v^*}{\partial x^{*2}}, \quad -\mathrm{Re}^2\frac{\partial p^*}{\partial r^*}$$

If these particular terms can be neglected, or canceled each other out, perfect agreement for the flow field should be found in terms of x^*, u^* and v^* for the same boundary conditions, irrespective of the Reynolds number. In Langhaar's analysis of the developing flow in a tube[8], the second derivative of velocity in the axial direction and the radial pressure gradient were neglected. Also, Pai and Hsieh[7] neglected all the pressure terms and the second derivative of the velocity gradient in the axial direction for the analysis of the free laminar jet and the laminar jet with free stream. Following their treatment, the terms listed above disappear for the cases of the 'free laminar jet' and 'developing laminar flow in a tube'. If we can assume that the sum of these terms containing Reynolds number is also small (or also increased in proportion to Re) for the conditions considered here, we can gain some insight as to the reason behind the lengthening of the flow field in approximate proportion to Reynolds number.

One would expect these three terms to be largest at the very entrance to the tube – which may explain the differences in the dimensionless radial velocities near the entrance shown in Fig. 7.

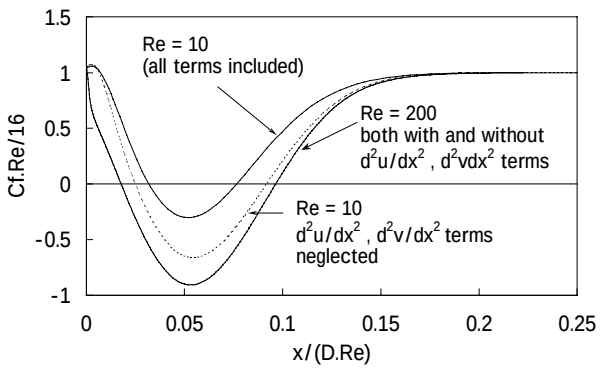

Fig. 9 Effect of neglecting second derivatives of velocity in the axial direction. (Solid lines – all terms included; dotted lines – second derivatives of velocity neglected. For Re = 200, the dotted line falls on top of the solid line).

Quite clearly, for creeping flow conditions the second derivative velocity terms containing Re in Eqs. (10) and (11) cannot be neglected, as the size of these terms may increase in proportion to the inverse square of Reynolds number.

Figure 9 shows the effect of neglecting the second derivatives of velocity in the axial direction. For Re = 10, the effect is remarkable but for Re = 200 the terms have negligible effect on the wall friction coefficient. Hence, the increasing importance of these terms explains why the recirculation disappears as Reynolds number becomes very small.

9. Practical Implications

Presently at the authors' laboratory of Kyoto University a multiple jet can-type combustor is being investigated for micro applications. Figure 10 shows a possible inlet geometrical configuration for the miniature combustion chamber. The fuel enters through the jet at the center and air through the surrounding six jets. Should such a device be suitably designed to operate under low Reynolds number laminar flow conditions, the present results would have a number of implications.

Figure 11 shows the calculated flow and mixing patterns for the inlet geometry illustrated in Fig. 10. Three Reynolds number cases are considered – Re = 50, 100 and 200. For all cases, the ratio of the primary and secondary mass flows is identical (m_1/m_2 = 0.0465). This value corresponds to the mass flow rates for a methane-air flame with an equivalence ratio of 0.8. Calculations were performed for constant density three-dimensional laminar flow. The selected plane in the θ direction is between two adjacent secondary stream jets.

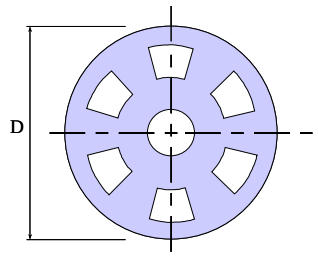

Fig. 10 Possible inlet configuration for multiple jet miniature can-type combustor.

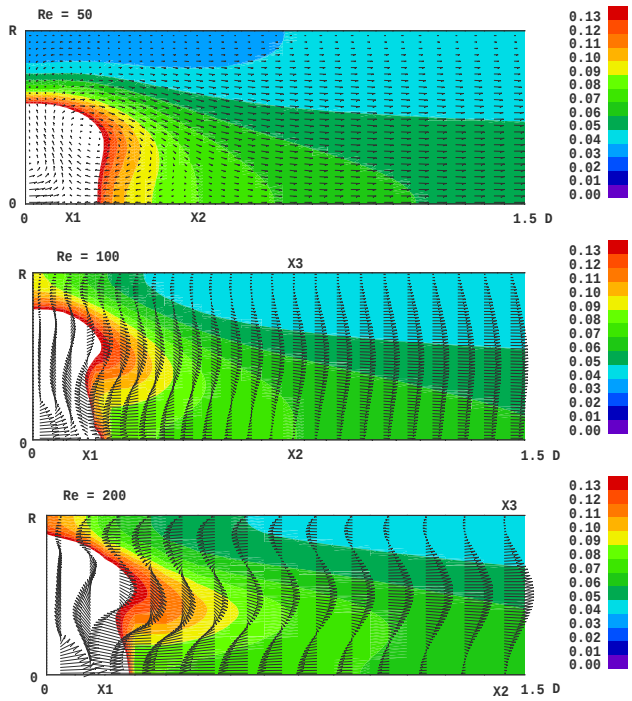

Fig. 11 Flow and mixing patterns for geometry given in Fig. 10 (Contours represent mass fraction of gas originating in the primary (center) jet: X1 = upstream stagnation point, X2 = downstream stagnation point, and X3 = Reattachment point of recirculation near wall).

The flow field shown in Fig. 11 is very complex with recirculation zones near the center of the tube and near the tube wall. In front of the primary jet a stagnation point, X1, appears. Further downstream, another stagnation point, X2, appears, which is also associated with the recirculation at the center. The position 'X3' gives the reattachment point for the recirculation at the wall of the tube. For the Re = 50 case, the flow pattern near the wall is different to the other cases so 'X3' is not marked.

In Fig. 11, the effect of changing Reynolds number from 100 to

200 is to move the positions 'X2' and 'X3' further downstream roughly in proportion to the Reynolds number. The upstream stagnation point, 'X1', however, moves only slightly with an increase in the flow rate for all three cases. This is perhaps because the second derivatives of velocity are very important in this region.

The change in the patterns of both velocity and mass fraction for the Re = 50 case in the vicinity of wall are further evidences of the low Reynolds number effects discussed in this paper.

10. Conclusions

1. While the 'Craya-Curtet' number appears to be an important parameter for the co-axial confined laminar jet, Reynolds number also plays a key role.
2. The primary effect of Reynolds number on the laminar cases investigated is to expand the flow field in the downstream direction with an increase of the Reynolds number. Close proportionality with Reynolds number has been demonstrated for the co-axial confined jet with recirculation (Ct = 0.4) for Reynolds number ranging from 50 to 200 (based on the outer tube diameter and bulk mean velocity).
3. In the low Reynolds number limit, the recirculation zone disappears for a Reynolds number between 5 and 10 under the Craya-Curtet number of 0.4. This is shown to be connected with an increasing importance of the second derivatives of velocity in the axial direction at such low Reynolds numbers.

Acknowledgement

This numerical work is one of the results of "Micro Gas Turbine / Fuel Cell Hybrid-Type Distributed Energy System" which is supported by Department of CREST in the program of JST.

References

1. Patankar, S. V., "Numerical Heat Transfer and Fluid Flow," Hemisphere Publishing Corporation, (1980).
2. Shavit, G. and Lavan, Z., "Analytical and experimental investigations of laminar mixing of confined heterogeneous jets," AIAA Journal, **11** (1973), pp. 352-358.
3. Kang, Y. M., "A Study on Heat Transfer in Recirculating Flows," PhD thesis, Kyoto University, (1980).
4. Rajaratnam, N., "Turbulent Jets," Elsevier Scientific Publishing Company, (1976).
5. White, F. M., "Viscous Fluid Flow," McGraw-Hill Inc., (1974).
6. Macagno, E. O. and Hung, T., "Computational and experimental study of a captive annular eddy," Journal of Fluid Mechanics, **28** (1967), pp. 43-64.
7. Pai, S. I. and Hsieh, T., "Numerical solution of laminar jet mixing with and without free stream," Applied Scientific Research (The Hague), **27** (1972), pp. 39-62.
8. Langhaar, H. L. "Steady flow in the transition length of a straight tube," *Trans. ASME*: Journal of Applied Mechanics, **64** (1942), pp. A55-A58.